Applied Surface Science 372 (2016) 20–29

Contents lists available at ScienceDirect

Applied Surface Science

journal homepage: www.elsevier.com/locate/apsusc

ZnO nanoparticles obtained by pulsed laser ablation and their composite with cotton fabric: Preparation and study of antibacterial activity

Valery Svetlichnyi, Anastasiia Shabalina *, Ivan Lapin, Daria Goncharova, Anna Nemoykina

Tomsk State University, 36 Lenina Ave., Tomsk 634050, Russian Federation

ARTICLE INFO

Article history:
Received 23 November 2015
Received in revised form 17 February 2016
Accepted 6 March 2016
Available online 8 March 2016

Keywords:
Zinc oxide
Nanoparticle
Pulsed laser ablation
Antibacterial activity
Cotton fabric

ABSTRACT

A simple deposition method was used to prepare a ZnO/cotton fabric composite from water and ethanol dispersions of ZnO nanoparticles obtained by the pulsed laser ablation method. The structure and composition of the nanoparticles from dispersions and as-prepared composites were studied using electron microscopy, X-ray diffraction, and spectroscopy. The nanoparticles and composite obtained exhibited antibacterial activity to three different pathogenic microorganisms—*Escherichia coli*, *Staphylococcus aureus*, and *Bacillus subtilis*. An attempt to understand a mechanism of bactericidal effect of ZnO nanoparticles was made. It was shown that zinc ions and hydrogen peroxide were not responsible for antibacterial activity of the particles and the composite, and surface properties of nanoparticles played an important role in antibacterial activity of zinc oxide. The proposed composite is a promising material for use as an antibacterial bandage.

1. Introduction

Semiconductor nanosized particles are widely used in different fields such as optoelectronics, catalysis, and sensorics. One of such materials is a wide-gap semiconductor (band gap of 3.37 eV), zinc oxide [1]. One more prospective application of ZnO is in biomedicine. Among antimicrobial agents, inorganic so-called "nanoantibiotics" [2] have attracted more and more attention. They exhibit great stability, high activity at low concentrations, and long shelf-life [3–5]. Zinc oxide is known as one of the most promising inorganic antibacterial agents. ZnO was found to demonstrate strong antibacterial and antifungal activity [6–10]. It was also shown [11] that after contact with ZnO slurry the sensitivity of *Escherichia coli* to some organic antibiotics increased. In addition, ZnO nanoparticles are active at pH values from 7 to 8 [12], which is suitable for use in water for washing and drinking. But despite the abundance of research in this area, the mechanism of antibacterial action of the zinc oxide is still not completely investigated [5,9,11].

ZnO nanoparticles can be used for disinfection purposes not only in the form of dispersions but also as a component of different materials, for example as filler for polymer film or as a coating [13]. Different materials covered with ZnO have been reported, including polymers [14], nano-fiber [15], silk [16], wool fibers [17], and cotton fabric [18–22]. It seems that antibacterial bandages based on different materials covered with ZnO nanoparticles have a great potential for hygienic and medical applications. Cotton fabric has many advantages in this area, such as natural composition, hypoallergenicity, and accessibility, and also it is an air penetrable material. Thus, this material is a very attractive as a basis for bandages containing ZnO.

The method that is the most frequently used for obtaining ZnO/cotton fabric composites is *in situ* synthesis of zinc oxide on the surface of the fabric. Zinc nitrate [18,20,23], zinc acetate [24], and zinc sulfate [21] are usually used as the source of zinc. Moreover, there is research in which pre-prepared ZnO was deposited on the cotton fabric from its dispersions using a pad-dry cure method [19,23] or layer-by-layer deposition [22]. In our opinion, using pre-prepared nanoparticle dispersions for obtaining ZnO/cotton fabric composites is more attractive from the practical point of view, since it does not require as precise control of the conditions as *in situ* methods require.

One of the main problems with using nanoparticle dispersions for biological and medical applications is purity of the material. Stabilizers and other additives are commonly used to obtain stable

* Corresponding author.
E-mail address: shabalinaav@gmail.com (A. Shabalina).

http://dx.doi.org/10.1016/j.apsusc.2016.03.043
0169-4332/

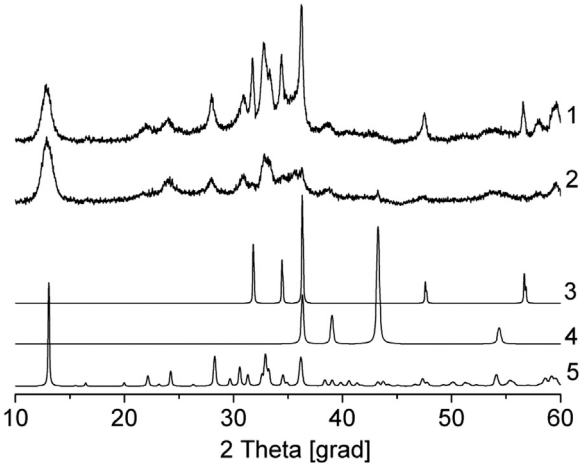

Fig. 1. XRD patterns for ZnO nanoparticles obtained by pulsed laser ablation in water (1) and ethanol (2); diffraction patterns from the International Centre for Diffraction Data: (3) ZnO (wurtzite), space group number 186, PDF Card #00-036-1451; (4) Zn, space group number 196, PDF Card #00-001-1244; (5) $Zn(CO_3)_2(OH)_6$, space group number 12 [30].

nanoparticle dispersions. But they can affect the properties of the composite obtained. Some authors [25–27] suggest using "green synthesis" for obtaining nontoxic, bio-safe and bio-compatible ZnO nanoparticles via environmentally friendly techniques using bio-organic reagents from plants. We proposed to obtain ZnO nanoparticle dispersions by the pulsed laser ablation method (PLA). PLA allows preparing nanoparticles in the form of stable dispersions in pure liquids without using additional chemical agents [28,29], which is very important for the subsequent utilization of the dispersions in biomedicine. Also, we proposed using a simple deposition method of ZnO nanoparticles from their dispersions onto the cotton fabric surface that is convenient and cheap.

Thus, the aim of the present work is the preparation of ZnO nanoparticle dispersions in liquids by the pulse laser ablation method; obtaining a new nano-ZnO/cotton fabric composite; the study of the antibacterial activity of both dispersions and composite; and the investigation of the mechanism of ZnO nanoparticle bactericidal effect.

2. Materials and methods

2.1. Preparation and characterization of nano-ZnO dispersions

ZnO nanoparticle dispersions were obtained by the pulsed laser ablation method as described in our previous article [30]. The metallic zinc target (99.9%) was immersed in a glass cylindrical vessel of 50 mL. Two pure solvents for colloids were used: distilled water and ethanol. The irradiation of the fundamental harmonic of Nd:YAG laser (LS-2132UTF, LOTIS TII, Belarus) was used (wavelength 1064 nm, pulse duration 7 ns, pulse energy 200 mJ, pulse repetition rate 15 Hz). The irradiation was focused by a short-focus lens F = 50 mm at the target surface through the transparent side wall of the glass reactor. To achieve uniform irradiation of the target, it was moved in the plane XY, perpendicular to the optical axis by means of two linear translators 8MT173-100 (Standa Ltd., Lithuania). Irradiation lasted for 30 min. Concentration of the dispersions was calculated on the basis of Zn target weight loss and was in the range of 0.5–0.6 g L^{-1}.

The nanoparticles obtained were studied by deposition of particles from dispersions onto carbon film on a copper grid and examination on a transmission electron microscope (TEM) CM 12 (Philips, Netherlands). X-ray diffractograms were recorded on XRD 6000 (Shimadzu, Japan). BET surface area was measured using TriStar II 3020 gas adsorption analyzer (Micromeritics, USA). The pH of liquid samples (23 °C) was measured with a pH-meter pH-150MI (Izmeritelnaya Technika Ltd., Russia). Zn^{2+} concentration was measured by stripping voltammetry using P-8nano (LLC Elins, Russia) potentiostat-galvanostat (3 electrodes: Ag/AgCl with 1 M KCl, Pt plate, and cylindrical glassy carbon). Before the voltammetric test of ZnO particle dispersion, the particles were separated from the solution.

2.2. Preparation of nano-ZnO/fabric composite

A piece of cotton fabric (density 110 g m^{-2}) of the size 10 × 10 cm was stretched on needle holders. The dispersion of ZnO (water or ethanol) was applied on the fabric by pipette until the whole piece was wetted. Then, the fabric was dried in a flat position using a heater with blowing air temperature of 50 °C. The procedure of wetting and drying was repeated to achieve the desired concentration of ZnO particles per cm^2. To keep the covering of the cotton fabric piece homogeneous, it was turned upside down from time to time. Nano-ZnO/fabric composites with the following concentrations were prepared: 0.05; 0.06; 0.08; 0.1; 0.2; 0.4; 0.6; 1 mg cm^{-2}.

2.3. Characterization of the composite

Optical micrographs were collected using Multiscope (LOMO, Russia). Scanning electron microscopy (SEM) data were obtained on Quanta 200 3 D (FEI Company, USA), 20 kV. Spectral-luminescence properties of the material were studied using Spectrophotometer Cary100 (Varian, USA) and Spectrofluorometer CM 2203 (SOLAR, Minsk, Belarus). Absorbance was investigated in the region of 200–900 nm, and fluorescence in the region of 220–820 nm. A unit with a diffuse reflectance photometric sphere was used to record absorbance spectra of the composite. The measurements were conducted in comparison with bare cotton fabric. A unit for solid samples with reflectance geometry was used to obtain fluorescence spectra and fluorescence excitation spectra.

2.4. Study of antibacterial activity of particle dispersions

For antibacterial experiments, *E. coli*, a Gram-negative bacterium, was selected as the main target organism. The culture *E. coli* B-6954 was obtained from the Russian Collection of Microorganisms. All materials were sterilized in an autoclave before the experiments. Meat-peptone broth was used for culturing the bacteria at 37 °C on an orbital shaker at a rotation speed of 200 rpm. The number of bacteria reached 2×10^9 CFU (colony forming units) per mL within 24 h.

The experiment with model liquid samples was conducted in order to study the possible mechanism of the antibacterial activity of ZnO nanoparticles. A supernatant of ZnO water dispersion was obtained via 21,000 rpm centrifugation for 60 min using Allegra 64R (Beckman Coulter, USA). ZnO micro-powder, $ZnCl_2$, and H_2O_2 obtained from Sigma-Aldrich were ACS reagent grade, and were used without additional purification. Concentrations of zinc-containing samples were specified for zinc (II) ions.

4.5 mL doses of the dispersions were placed in sterile tubes. 0.5 mL of *E. coli* culture, previously diluted with meat-peptone broth to the concentration of 3.0×10^6 CFU/mL, was added. Thus, the final concentration of bacteria in the dispersion was 3.0×10^5 CFU/mL. Samples were cultured in an incubator at 37 °C without agitation for 5 min (zero point), and 24 h. Then, 1 mL doses were diluted in 9 mL of 0.9% NaCl and thoroughly mixed. The dilution was repeated. Mixtures obtained (0.1 mL) were deposited on individual Petri dishes with Endo agar. Then the samples were incubated for 24 h at 37 °C, and the number of grown colonies was counted and compared with the control sample.

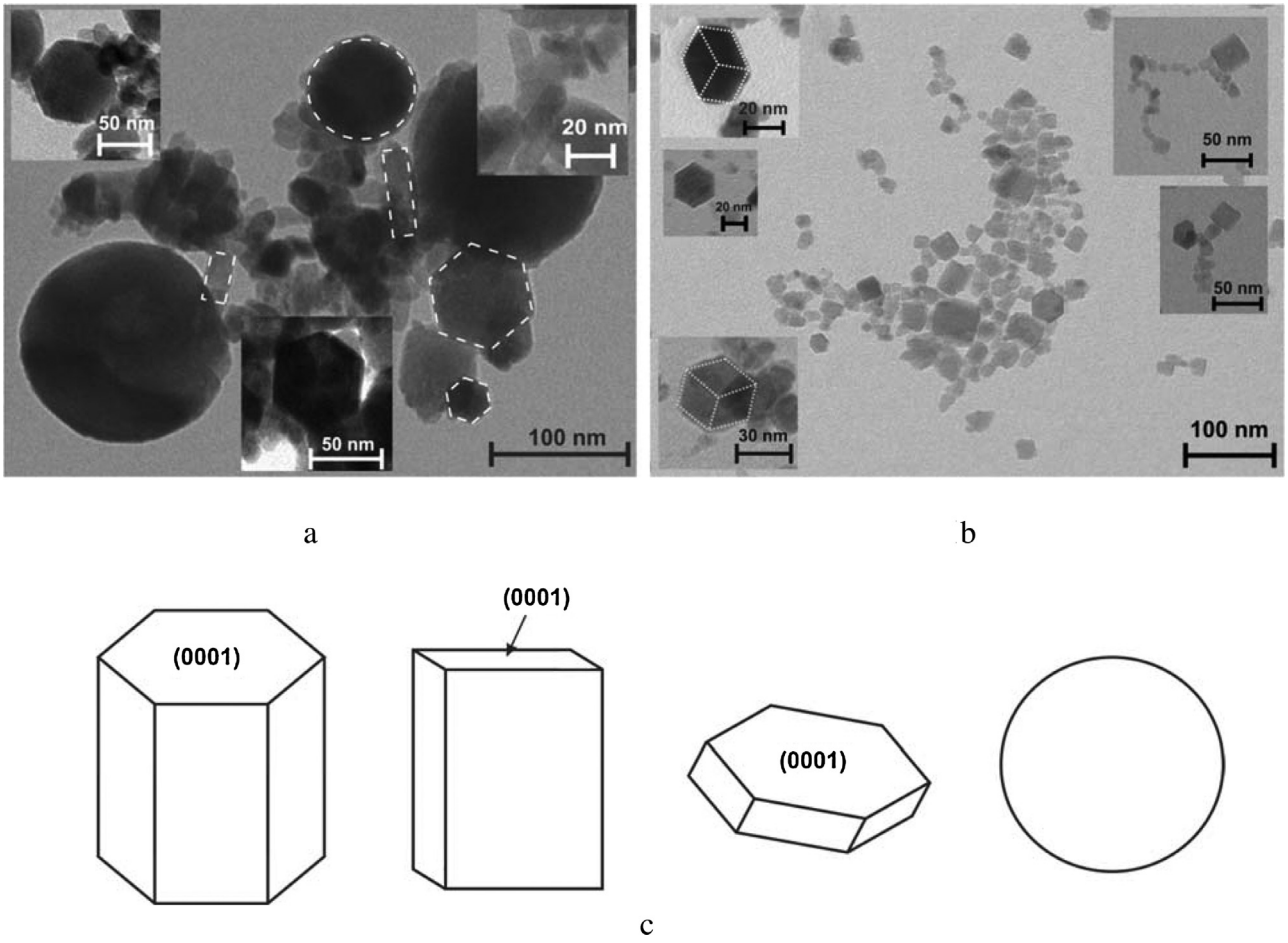

Fig. 2. TEM images for ZnO nanoparticles obtained by pulsed laser ablation in water (a) and ethanol (b); (c) possible forms of ZnO crystals.

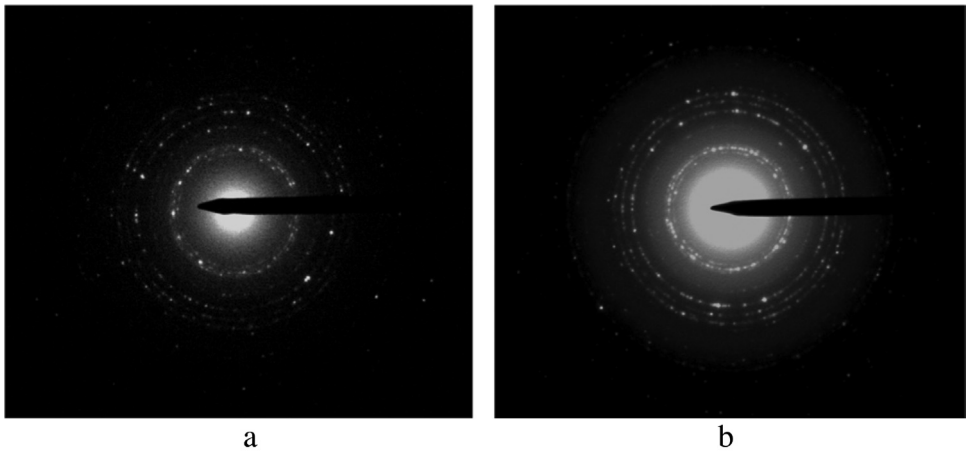

Fig. 3. SAED patterns for ZnO particles from water (a) and ethanol (b) dispersion.

The same experiment with dispersions of nanoparticles of different metals was carried out. The final concentration of bacteria was $3–6 \times 10^2$ CFU/mL.

2.5. Study of antibacterial activity of the composite

E. coli was added to the sterile molten meat-peptone agar at 40°. The suspension was stirred and poured in the dishes (20 mL at each), and 3 fabric composite samples (10×10 mm) were immersed in each. Thus, the whole sample is in contact with the agar. (When placed on top of the agar the sample does not adhere to the surface. Therefore, it was decided to dip the cloth in the molten agar.) The final number of bacteria in the deep seeding was 10^5 CFU mL^{-1}. Dishes with the solidified agar were inverted and incubated at 37 °C. Five Petri dishes with three samples for each variant were used in the experiment. Inhibition zones were measured after 18 h. The average width of the inhibition zone was calculated using the formula:

$$W = (T - D)/2,$$

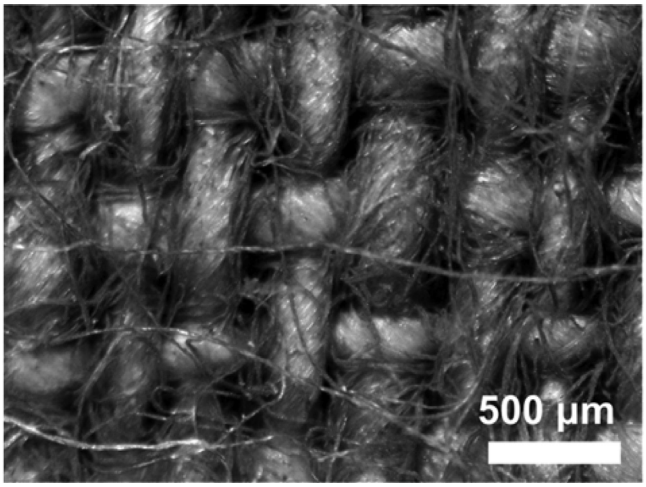

Fig. 4. Optical micrograph for bare cotton fabric.

where W is a width of the clear zone of inhibition, in millimeters; T is the overall diameter of the inhibition zone, mm; and D is the sample size, mm.

Two more bacteria were used to assess the antibacterial effectiveness of nano-ZnO/fabric composite: *Staphylococcus aureus* (Gram-positive), and *Bacillus subtilis* (Gram-positive, spore-forming). These bacteria were grown and diluted using the same protocol as was used with the *E. coli*.

The same experiment with cotton fabric samples impregnated (according to the procedure described above) by other model liquids was conducted in order to understand the mechanism of the antibacterial activity of ZnO nanoparticles. The first model sample–micro-ZnO/fabric–was obtained from the water dispersion of ZnO micro-powder (Sigma-Aldrich), and the same concentration was taken as for the nano-ZnO dispersion. The second model system–supernatant/fabric–consisted of cotton fabric impregnated by supernatant (see previous section). The third model composite–$ZnCl_2$/fabric–was prepared from zinc (II) chloride solution with the same mass concentration of zinc as it was in the nano-ZnO dispersion.

3. Results and discussion

3.1. Characterization of ZnO nanoparticles

Similar ZnO dispersions in water and ethanol were characterized in our previous work [30]. XRD has shown (Fig. 1) that particles from water dispersion consisted of ZnO and $Zn(CO_3)_2(OH)_6$, and that powder from ethanol dispersion contained only ZnO (99%) and metallic zinc. In the present work, all the dispersions after preparation were bubbled by air (15 min, gas flow rate of 1–3 L min^{-1}) in order to stimulate the oxidation process and obtain only one phase–hexagonal ZnO (wurtzite).

Fig. 2a and b shows TEM images of nanoparticles obtained. As one can notice, ZnO particles in water dispersion are more strongly aggregated in comparison with the ethanol dispersion. Also it is seen that the nanoparticles have different forms when obtained in different solvents. It is well known that the form of ZnO crystallites depends on the conditions of synthesis. In work [31] the authors obtained hexagonal rods and hexagonal plates (Fig. 2c, first and third structures from left to right) by partial blocking of (0 0 0 1) plane in wurtzite crystal, which changed the habit of crystal growth. Using the same approach, the authors [32] obtained four different structures of ZnO crystallites, including flat square plates (Fig. 2c, second structure from left to right). Spherical zinc oxide particles

Table 1
Selected area diffraction (SAED) results and parameters from crystallographic database PDF-4.

d_{SAED}	d_{PDF}	hkl	Intensity	Description
2.83768	2.8143	100	57	ZnO wurtzite type
2.62241	2.6033	002	44	PDF Card #00-036-1451
2.469152	2.4759	101	100	Space group P63mc (186)
1.920452	1.9111	102	23	Lattice constants:
1.639006	1.6247	110	32	a = b = 3.250 Å, c = 5.207 Å,
1.485349	1.4771	103	29	α = β = 90°, γ = 120°
1.387772	1.3782	112	23	

can also be obtained during spray pyrolysis [33] or vapor deposition [34] processes. In the case of pulsed ablation there are at least three forms of crystallites in the sample obtained in water (Fig. 2a). Spherical particles have the largest size among the structures (up to 150 nm). The hexagons are almost uniform in size; they show diameters from 50 to 80 nm. The smallest particles–rods–are 10–30 nm in width and up to 70 nm in length. ZnO particles obtained in ethanol demonstrate a completely different picture. They mostly consist of flat square plates from 10 to 60 nm (Fig. 2b). Hexagons can also be found, but there is no strong confidence in their hexagonal form; they may be only thicker plates that grew to cuboids (see insets Fig. 2b). Since pulsed laser ablation was conducted in the absence of any chemical additives, these forms of ZnO particles can be explained only by interaction of the target material with the solvent under radiation. This issue is beyond the scope of this study and requires deeper research.

Fig. 3 shows selected area electron diffraction (SAED) patterns for ZnO nanoparticle agglomerates. Patterns are of a polycrystalline type, and the seven brightest rings were found to belong to ZnO wurtzite (see Table 1). Thus, additional air bubbling resulted in complete oxidation of particles to zinc oxide.

BET surface area of nano-ZnO powders obtained was found to be 19.3 and 25.9 $m^2 g^{-1}$ for samples from water and ethanol dispersions, respectively.

3.2. Characterization of nano-ZnO/fabric composite

An optical micrograph of the cotton fabric is presented in Fig. 4. The fabric consists of individual fibers that form bundles (about 250 μm) with simple interlacing in perpendicular directions.

SEM-images on Fig. 5a–d shows individual bundles without ZnO and bundles of nano-ZnO/fabric composite with different concentrations of ZnO impregnated from water dispersions obtained by PLA. Zinc oxide particles and their agglomerates cover the fibers of the fabric, which is clearly seen from SEM-images with z-contrast (Fig. 5c and d), where the heavier atoms of metal shine more brightly than the fiber. It is clear that the degree of coverage depends on the concentration of deposited nano-ZnO. But it is seen that in all the cases, the covering of fibers by nanoparticles and their agglomerates is fairly uniform.

The composite was studied by the XRD method (Fig. 6). Reflexes in the angles before 25° belong to the components of the fabric. It can be seen that zinc (II) oxide is a major crystal phase in the samples after deposition on cotton fabric from both water and ethanol. Moreover, it is the only phase in the sample obtained by impregnation from water dispersion. About 6% of hexagonal Zn is present on the surface of the composite when ethanol dispersion was used. Probably, metallic Zn is situated in the cores of ZnO nanoparticles that have not been oxidized completely. The average crystallite size of the zinc oxide is 13–15 nm, but for metallic zinc it is about 24 nm. This might be indirect evidence of the fact that the cores of the largest particles consist of non-oxidized Zn.

The presence of zinc oxide is confirmed by the data from the absorption spectroscopy (Fig. 7) and the UV–vis fluorescence spec-

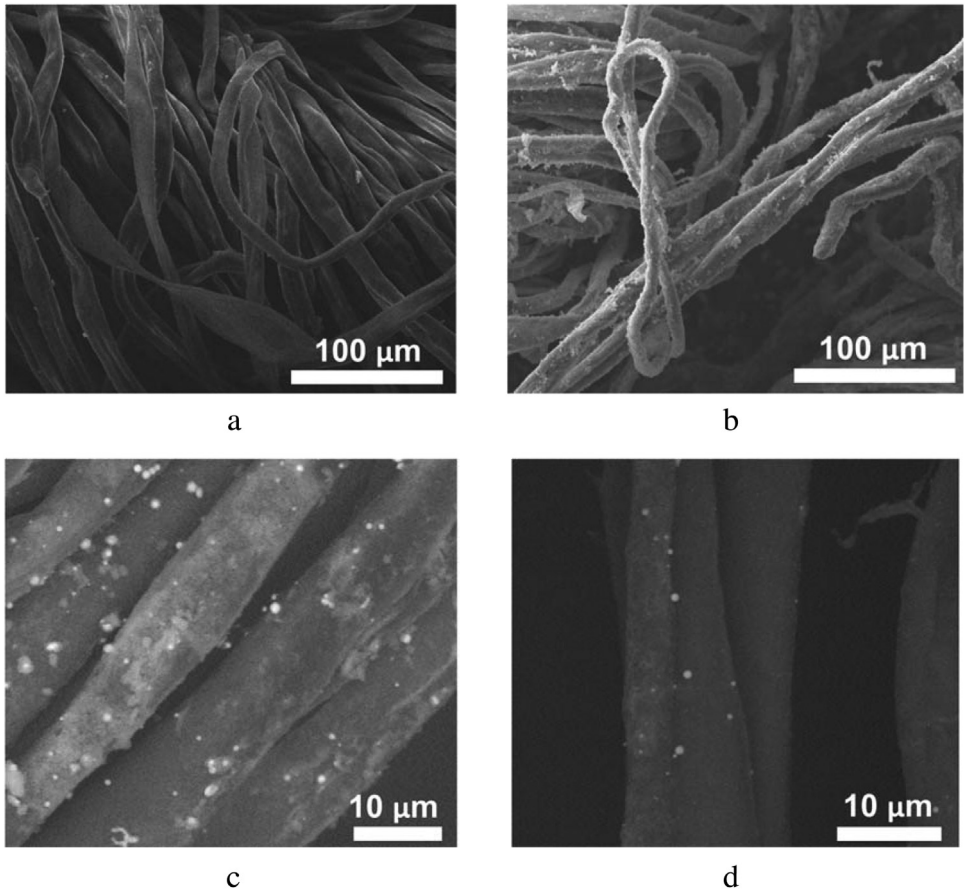

Fig. 5. SEM-data for bare cotton fabric (a) and nano-ZnO/fabric composite (c-d) with ZnO content of 1 mg cm^{-2} (b, c), 0.1 mg cm^{-2} (d). Images (a) and (b) were collected using secondary electrons, and (c) and (d) were recorded using back-scattered electrons (z-contrast mode).

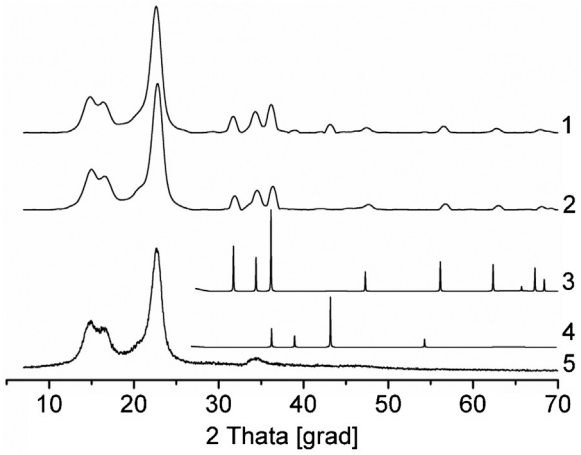

Fig. 6. X-ray diffractograms of nano-ZnO/cotton fabric composites obtained from water (1) and ethanol (2) dispersions, and diffractograms from the database of the International Centre for Diffraction Data for ZnO, wurtzite #00-036-1451 (3), Zn, #00-001-1244 (4), and diffractogram of bare cotton fabric (5).

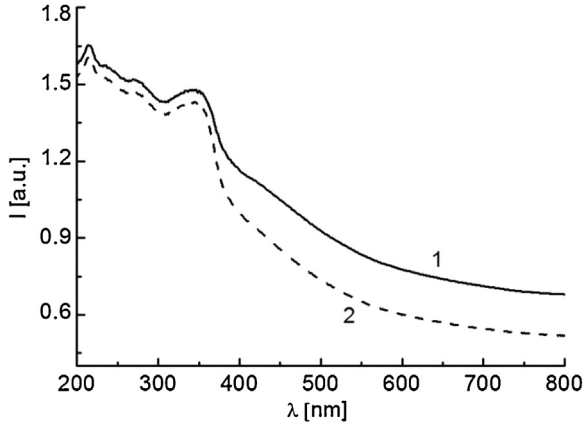

Fig. 7. Absorption spectra of ZnO/fabric composite from water (curve 1) and ethanol (curve 2) dispersions, Zn content 0.6 mg cm^{-2}.

troscopy (Fig. 8). So, the absorption spectra of ZnO/fabric composite (Fig. 7) clearly shows the peak of the exciton absorption at 360 nm, which is the same as, for example, that in [27].

Spectra of fluorescence and of excitation fluorescence give additional information (Fig. 8). Bare cotton fabric has an emission peak with a maximum at 430 nm ($\lambda_{excitation}$ = 310 nm). The study of excitation fluorescence spectra at registration wavelength of 450 nm has shown that this fluorescence is formed by the substance with a maximum of absorbance at 380 nm. These spectral properties of the bare fabric belong to a whitener that is used in the fabric production. After the deposition of nanoparticles on the fabric, a peak at 640 nm appeared that belonged to the luminescence of ZnO defective states [30]. Using records of fluorescence excitation spectra with registered emission at 640 nm, it was established that this radiation belongs to the absorption at 360 nm. And this absorption belongs to ZnO [30]. Thus, these results both confirm the presence of ZnO in the composite, and denote its high degree of defectiveness. As noted in [27], the emissions of ZnO described

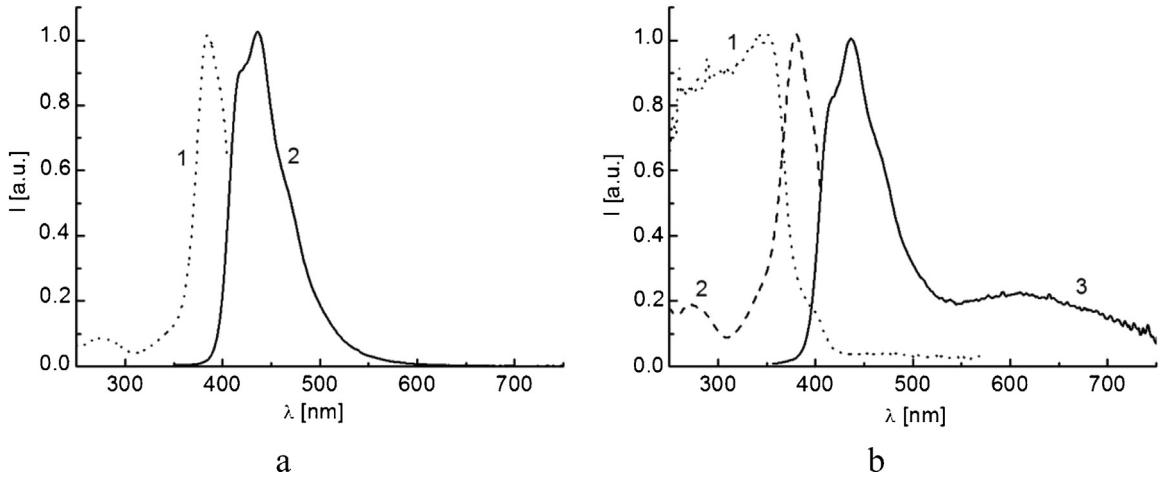

Fig. 8. Spectra of fluorescence excitation ($\lambda_{emission}$ = 630 nm)—curve 1, ($\lambda_{emission}$ = 430 nm)—curve 2, and spectra of fluorescence emission ($\lambda_{excitation}$ = 310 nm)—curve 3, for bare cotton fabric (a) and for nano-ZnO/fabric 1 mg cm^{-2}, obtained from ethanol dispersion (b).

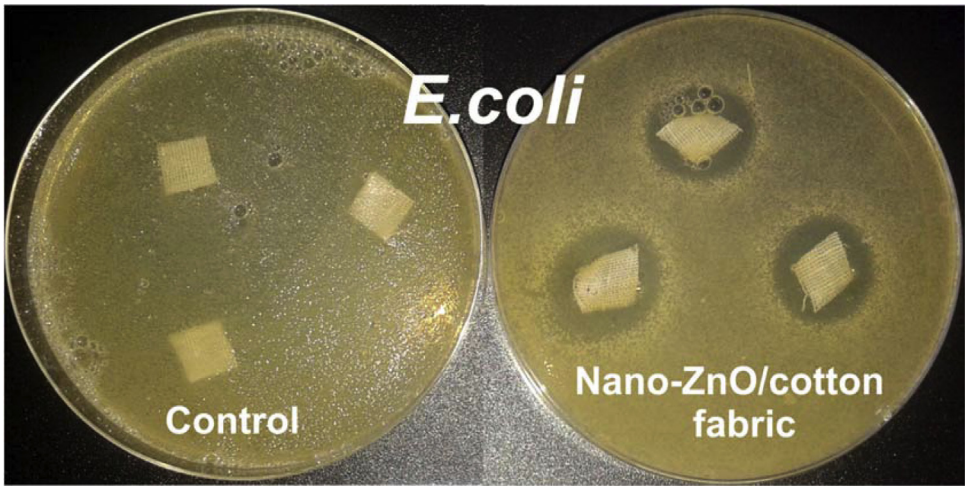

Fig. 9. Photos of the sample s in agar with *E. coli* after 24 h: control sample of bare cotton fabric; nano-ZnO/fabric composite (0.2 mg cm^{-2}) obtained from water dispersion.

above are highly desirable because they can find application in light emitting and biological fluorescence labeling.

3.3. Study of antibacterial activity of particle dispersions

Antibacterial activity of ZnO water dispersion was tested along with distilled water in a parallel test, and with dispersions of nanoparticles of noble metals (Au, Pt, Ag) obtained by PLA. Table 2 represents the results obtained. One can notice that ZnO water dispersion Exhibits 100% bactericidal effect under the experimental conditions. Silver nanoparticles are known as a strong antibacterial agent, but their activity was found to be lower.

3.4. Antibacterial activity of nano-ZnO/fabric composite

Inhibition zone (a zone of inhibition) is an area around the sample where the bacteria have not grown enough to be visible. On Fig. 9 there are photographs of the inhibition zones for the control sample and the nano-ZnO/fabric composite. It is seen that in the absence of Zn-containing additions, the cotton fabric is completely covered with colonies of *E. coli*. It also can be seen that an inhibition zone appeared around nano-ZnO/fabric composites. Thus, ZnO nanoparticles obtained by laser ablation on the cotton fabric kill bacteria and/or inhibit their growth.

Fig. 10 shows the dependence of the inhibition zone size on the nano-ZnO concentration in the composite. It is noticeable that antibacterial effect appears only after an increase in ZnO concentration up to 0.1 mg cm^{-2} for composites obtained from both water and ethanol dispersions. Also, it should be noted that rapid increase of the inhibition zone diameter at the minimal concentration of zinc oxide is replaced by a slow increase during the following growth of ZnO content.

Generally, composites obtained from ethanol dispersions show larger inhibition zones than those obtained from water dispersion. In both cases the composition of the surface of the nanoparticles is the same (metallic Zn present in the center of particles from ethanol dispersion that does not interact with bacteria). That is why it was suggested that mobility of nanoparticles may cause this difference. The mobility is connected with the size of agglomerates and the strength of the particles' fixation on the fabric surface. To study the possible influence of ZnO particles' mobility on *E. coli* growth inhibition zone diameter, an experiment with additional wetting of the composite fabric was conducted. It was found that wetting increased the diameter of the inhibition zone from 20.00 ± 1.5 up to 22.50 ± 0.7 mm for ethanol-originated composite (0.2 mg cm^{-2}), and from 15.62 ± 1.07 up to 18.00 ± 0.8 mm for water-originated composite (0.2 mg cm^{-2}). It is seen that wetting leads to an increase of inhibition zone diameter by 10–20%. On the other hand, high

Table 2
Data on *E. coli* concentration change over 24 h in contact with liquid samples.

Sample	Concentration	Initial concentration of *E.coli*, CFU mL^{-1}	Concentration of *E.coli* after 24 h, CFU mL^{-1}
Distilled water	–	$5.8 \pm 0.18\ 10^2$	$3.6 \pm 0.13\ 10^3$
Nano-ZnO dispersion	50 mg L^{-1}	$5.6 \pm 0.25\ 10^2$	0
Au dispersion	50 mg L^{-1}	$3.0 \pm 0.31\ 10^2$	$3.2 \pm 0.51\ 10^3$
Pt dispersion	50 mg L^{-1}	$3.1 \pm 0.12\ 10^2$	$3.7 \pm 0.32\ 10^3$
Ag dispersion	50 mg L^{-1}	$2.7 \pm 0.27\ 10^2$	10^1

Table 3
Bacteria growth inhibition zones for nano-ZnO/fabric composite (1 mg/cm^2) obtained from ethanol dispersion.

Microorganism	W (dry sample), mm
Escherichia coli (Gram-negative)	26.83 ± 1.52
Staphylococcus aureus (Gram-positive)	17.90 ± 0.60
Bacillus subtilis(Gram-positive, spore-forming)	19.10 ± 0.49

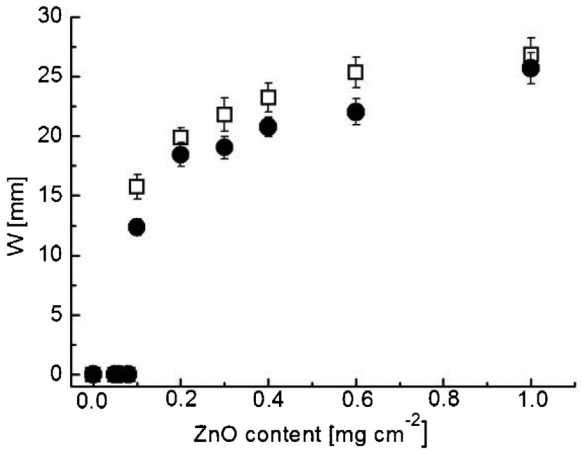

Fig. 10. Influence of nano-ZnO concentration on *E. coli* growth inhibition zone diameter. Square marks (□) for the composites obtained from ethanol dispersion of ZnO nanoparticles; circle marks (●) for the composites from water dispersion of ZnO particles.

localization of the bactericidal effect may be an advantage. For example, in the case of wound disinfection it is necessary to treat only the damaged area, without affecting non-damaged skin.

In addition to *E. coli*, two other pathogenic bacteria were used to estimate the antibacterial activity of nano-ZnO/fabric composites (Table 3). The study has shown that the composite exhibited antimicrobial activity against a wide range of pathogenic microorganisms, which is an important advantage.

Unlike many other authors ([20,22], for example) we did not study mechanical and UV-blocking properties of the composite obtained, along with laundering durability, because there are no such requirements for bandage materials.

3.5. Mechanism of ZnO antibacterial activity

Many studies of the possible antibacterial mechanism of ZnO nanoparticles have been done recently. The authors of [9,11,12,35] consider reactive oxygen species (ROS), including hydrogen peroxide and radicals, as the main mechanism of killing bacteria and inhibiting their growth. In the work [36] radical ROS were found in ZnO dispersion. Authors [14,37] suppose that zinc (II) ions are responsible for antibacterial activity of ZnO, even though [38] has shown that Zn^{2+} did not give the same bactericidal effect. Among other opinions is that there is an accumulation of nanoparticles themselves in bacteria cells [13], and mechanical damage to the bacteria cell membrane by ZnO particles [5]. Zhang et al. [39] conducted a complex experiment and disproved some of the above-mentioned suggestions. But the mechanism of ZnO antibacterial activity is still under discussion. The fact that the properties of nanoparticles strongly depend on the methods of their preparation makes the task even more complicated, since there might be no uniform mechanism for different ZnO particles, and also research approaches can be different. In this work we attempted to determine whether some of the suggested mechanisms are possible in the case under investigation.

Zinc (II) ions are present in nano-ZnO dispersions and also they can be formed in liquid medium due to dissolving the nanoparticles' surface. It is known that the nature of the experimental medium affects the zinc ions' mobility. That may be a reason why wet composites have shown greater antibacterial activity (see above, section 3.4)–water promotes release of zinc ions from the composite and their spreading more widely in the Petri dish.

In order to learn more of the mechanism of antibacterial activity of ZnO nanoparticles obtained by PLA, the following experiment was conducted. A supernatant of ZnO water dispersion was obtained by centrifugation. The concentration of zinc (II) ions in ZnO water dispersion and in its supernatant was measured by stripping voltammetry. The amount of $6.9(\pm 0.3) \times 10^{-4}$ M of Zn^{2+} was detected in ZnO dispersion, and $7.4(\pm 0.3) \times 10^{-4}$ M of Zn^{2+} was found in the supernatant. Thus, the content of zinc ions is the same in the dispersion and in the solvent after deletion of the nanoparticles. Hence, if Zn^{2+} ions are the main cause of the antibacterial activity of the ZnO dispersion, they would have been detected by using supernatant instead of nanoparticle dispersion. At the same time, zinc (II) chloride solution with a concentration of 50 mg L^{-1} (by Zn) was used as a model sample. An excessive concentration of Zn^{2+} was used to find whether zinc ions were responsible for ZnO's bactericidal effect. Another model solution contained hydrogen peroxide. According to [40] bulk concentration of H_2O_2 in ZnO powder dispersion (1 g L^{-1}) was approximately 0.5 mg L^{-1}. The authors [11] showed that the bactericidal effect of ZnO powder slurry was greater than that of hydrogen peroxide solution with corresponding concentration. Then they also used 0.31 g L^{-1} (0.0155 M) solution of H_2O_2. In the present study, the solution of hydrogen peroxide with the same concentration was used to compare its antibacterial activity with that of other samples.

An antibacterial experiment was performed using the same protocol (see Section 3.3) but with higher *E. coli* concentration. Table 4 shows the results obtained. It may be noticed that pH values were almost the same for supernatant, zinc chloride, and hydrogen peroxide solutions. And pH was a little more basic for distilled water and ZnO particle dispersions.

Higher concentration of bacteria requires more time to inhibit their growth. But it is still seen that even in this case, ZnO led to the decrease of the number of *E. coli*. This was true for both micro- and nano-particles. Zinc chloride solution and supernatant did not lead to the decrease in the order of the number of bacteria. Thus, the antibacterial activity of the zinc oxide particles was not mainly due to the release of zinc (II) ions. Also, hydrogen peroxide did not show bactericidal effect under experimental conditions. This fact denotes that ZnO nanoparticle activity is likely not based on H_2O_2 formation.

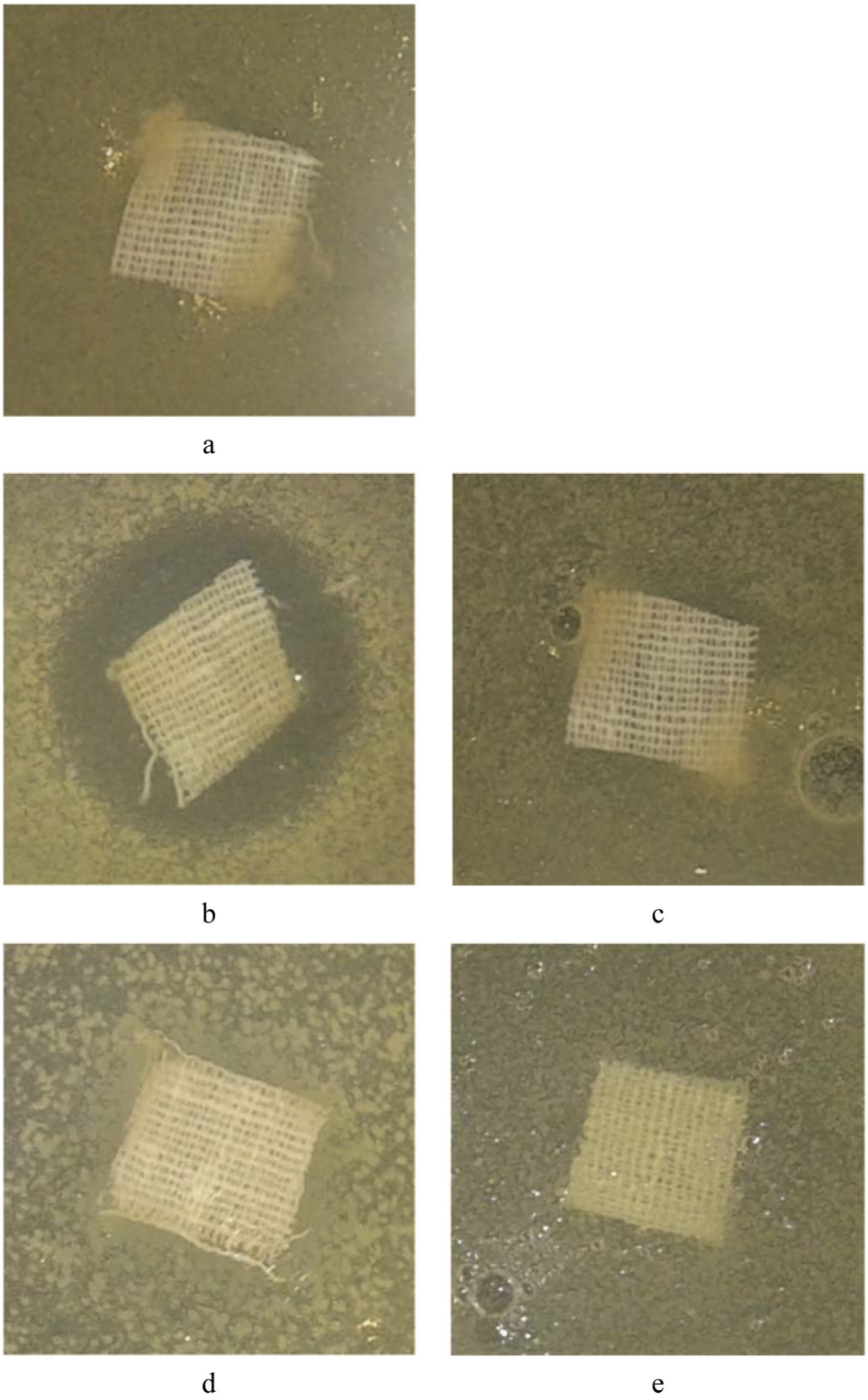

Fig. 11. Photos of the samples of fabric composites in agar with *E. coli* after 24 h: (a) bare cotton fabric; (b) nano-ZnO/fabric; (c) micro-ZnO/fabric; (d) supernatant/fabric; (e) $ZnCl_2$/fabric.

Thus, ZnO micro- and nano-particle dispersions have shown almost the same antibacterial activity against *E. coli*. Their activity presumably is not based on H_2O_2 formation or zinc (II) ion release.

To assess the role of zinc ions in the antibacterial mechanism of nano-ZnO/fabric composite, an experiment with cotton fabric impregnated with $ZnCl_2$ solution (sample "$ZnCl_2$/fabric"), and with supernatant of nano-ZnO dispersion (sample "supernatant/fabric") was performed. In addition, in order to establish the influence of ZnO particle size and nature on their activity, the sample "micro-ZnO/fabric" was prepared from micro-ZnO dispersion. The results of the activity of these materials in the experiment with *E. coli* are presented in Fig. 11.

Table 4
Data on *E. Coli* concentration change over 24 h in contact with liquid samples.

Sample	Concentration	pH	The number of *E.coli* in the co-culturing, CFU mL^{-1}	
			5 min	24 h
Distilled water	–	8.36	$(3.1 \pm 0.78)\cdot10^5$	$(8 \pm 1.24)\cdot10^5$
Nano-ZnO	50 mg L^{-1}	8.15	$(2.8 \pm 0.51)\cdot10^5$	$(3.0 \pm 0.90)\cdot10^4$
Micro-ZnO	50 mg L^{-1}	7.75	$(3.0 \pm 0.51)\cdot10^5$	$(4.0 \pm 0.82)\cdot10^4$
Supernatant	–	6.82	$(3.1 \pm 0.38)\cdot10^5$	$(5.1 \pm 0.80)\cdot10^5$
$ZnCl_2$	50 mg L^{-1}	6.75	$(3.2 \pm 0.70)\cdot10^5$	$(1.3 \pm 0.97)\cdot10^5$
H_2O_2	0.0155 M	6.80	$(3.0 \pm 0.50)\cdot10^5$	$(4 \pm 1.13)\cdot10^5$

A well-defined inhibition zone was seen around nano-ZnO/fabric composite. Also slight concentrational depletion of *E. coli* colonies could be noticed on the perimeter of the piece of micro-ZnO/fabric composite (Fig. 11c). No inhibition zones were seen for pieces impregnated from supernatant and zinc (II) chloride solution (Fig. 11d and e). Thus, it can be concluded that even though Zn^{2+} can have antibacterial activity, the mechanism of inhibition of bacteria growth in the case of nano-ZnO/fabric composite has a different nature.

Data in Fig. 11b and c show that the antibacterial mechanism of ZnO particles can be based only on the action of the nanoparticles themselves: either ROS form on their surface, or bacteria cells are mechanically damaged through their contact with particles. Both mechanisms are determined by surface properties of the particles, which depend on the particle size and defect structure. Nano- and micro-ZnO particles average 10 and 1000 nm, respectively. BET surface area is 19.3 $m^2\ g^{-1}$ for nano-ZnO, and 3.4 $m^2\ g^{-1}$ for micro-ZnO. Since nano-ZnO particles are smaller, it is easier for them to interact with bacteria cells and their membrane or even to penetrate it; this mechanism seems to be more likely. But at the same time nano-ZnO particles have a larger BET surface area than micro-ZnO and, consequently, nano-ZnO particles may cause more effective ROS formation. This may be true also because smaller particles have more a defective structure. Surface defects are known to be responsible for ROS formation on the surface of semiconductors. And, as has been shown, zinc oxide on the surface of nano-ZnO/fabric composite has a high degree of defectiveness. At the same time low activity of micro-ZnO particles may be connected with the lower mobility of larger particles in the medium. In this connection, the size of the particles is crucial. Thus, it is established that ZnO nanoparticles are active against bacteria, and this activity is not due to zinc (II) ions, but strongly connected with surface properties of ZnO particles.

4. Conclusion

In the present work nano-ZnO water and ethanol dispersions obtained by pulsed laser ablation were used to produce nano-ZnO/cotton fabric composite via simple nanoparticle deposition. The structure, composition, and antibacterial properties of the nanoparticles from dispersions and as-prepared composite were studied. It was shown that ZnO nanoparticles and nano-ZnO/fabric material exhibit antibacterial activity against three different pathogenic microorganisms. An attempt to understand a mechanism of bactericidal effect of ZnO nanoparticles was made. It was suggested that in the case under study, H_2O_2 and Zn^{2+} are not mainly responsible for antibacterial activity of zinc oxide. The results obtained point to the important role of surface properties of nanoparticles, their size and specific surface area. Thus, the objective of our further research is to study in detail the antibacterial mechanism for ZnO nanoparticles and to develop methods for improving the effectiveness of their application.

The nano-ZnO/cotton fabric composite proposed proved to be a promising material for use as an antibacterial bandage, since it shows bactericidal effect, does not contain chemical extra-additives, is easy to prepare from ZnO nanoparticle dispersion, and is also cheap.

Acknowledgements

This study was supported by the Tomsk State University Academic D.I. Mendeleev Fund Program (research grant # 8.2.57.2015).

References

[1] Z.L. Wang, J. Phys. Condens. Matter 16 (25) (2004) R829–R858.
[2] A.J. Huh, Y.J. Kwon, J. Control Release 156 (2011) 128–145.
[3] M. Rai, A. Yadav, A. Gade, Biotechnol. Adv. 27 (2009) 76–83.
[4] P.K. Stoimenov, R.L. Klinger, G.L. Marchin, K.J. Klabunde, Langmuir 18 (2002) 6679–6686.
[5] J. Sawai, J. Microbiol. Methods 54 (2003) 177–182.
[6] M. Eskandari, N. Haghighi, V. Ahmadi, F. Haghighi, S.R. Mohammadi, Phys. B 406 (2011) 112–114.
[7] M. Mirhosseini, F.B. Firouzabadi, Iran. J. Pathol. 9 (9) (2014) 99–106.
[8] K. Kairyte, A. Kadys, Z. Luksiene, J. Photoch, Photobiol. B. 128 (2013) 78–84.
[9] R.K. Sharma, R. Ghose, Ceram. Int. (2015), http://dx.doi.org/10.1016/j.ceramint.2014.09.016.
[10] O. Yamamoto, Int. J. Inorg. Mater. 3 (2001) 643–646.
[11] J. Sawai, S. Shoji, H. Igarashi, A. Hashimot, T. Kokugan, M. Shimizu, H. Kojima, J. Ferment. Bioeng. 86 (86) (1998) 521–522.
[12] O. Yamamoto, K. Nakakoshia, T. Sasamotoa, H. Nakagawa, K. Miura, Carbon 39 (2001) 1643–1651.
[13] M. Moritz, M. Geszke-Moritz, Chem. Eng. J. 228 (2013) 596–613.
[14] N. Vitchuli, Q. Shi, J. Nowak, K. Kay, J.M. Caldwell, F. Breidt, M. Bourham, M. McCord, X. Zhang, Sci. Technol. Adv. Mater. (2011), http://dx.doi.org/10.1088/1468-6996/12/5/055004.
[15] Y. Gao, Y.B. Truong, Y. Zhu, I.L. Kyratzis, J. Appl. Polym. Sci. (2014), http://dx.doi.org/10.1002/APP.40797.
[16] J. Xu, H. Su, J. Han, Y. Chen, W. Song, Y. Gu, W.J. Moon, D. Zhang, Appl. Phys. A 108 (2012) 235–238.
[17] A. Behzadnia, M. Montazer, M.M. Rad, Ultrason. Sonochem. 27 (2015) 200–209.
[18] D. Staneva, D. Atanasova, E. Vasileva-Tonkova, V. Lukanova, I. Grabchev, Appl. Surf. Sci. 345 (2015) 72–80.
[19] K.B. Yazhini, H.G. Prabu, Appl. Biochem. Biotechnol. 175 (2015) 85–92.
[20] M. Shateri-Khalilabad, M.E. Yazdanshenas, Text. Res. J. 83 (10) (2013) 993–1004.
[21] I.M. El-Nahhal, S.M. Zourab, F.S. Kodeh, A.A. Elmanama, M. Selmane, I. Genois, F. Babonneau, Mater. Sci.: Mater. Electron. 24 (2013) 3970–3975.
[22] S.S. Ugur, M. Sariisik, A.H. Aktas, M.C. Ucar, E. Erden, Nanoscale Res. Lett. 5 (2010) 1204–1210.
[23] Y. Li, Y. Zou, D. An, Y. Hou, Q. Zhou, L. Zhang, Fiber Polym. 14 (6) (2013) 990–995.
[24] S. Shahidi, L. Zarei, S.M. Elahi, Fiber Polym. 15 (12) (2014) 2472–2479.
[25] K. Elumalai, S. Velmurugan, S. Ravi, V. Kathiravan, S. Ashokkumar, Mater. Sci. Semicond. Process. 34 (2015) 365–372.
[26] M. Stan, A. Popa, D. Toloman, A. Dehelean, I. Lung, G. Katona, Mater. Sci. Semicond. Process. 39 (2015) 23–29.
[27] K. Elumalai, S. Velmurugan, Appl. Surf. Sci. 345 (2015) 329–336.
[28] Z. Yan, D.B. Chrisey, J. Photochem. Photobiol. C 13 (2012) 204–223.
[29] H. Zeng, X.W. Du, S.C. Singh, S.A. Kulinich, S. Yang, J. He, W. Cai, Adv. Funct. Mater. 22 (2012) 1333–1353.
[30] V.A. Svetlichnyi, I.N. Lapin, Russ. Phys. J. 56 (5) (2013) 581–587.
[31] Y.V. Kaneti, Z. Zhang, J. Yue, Q.M.D. Zakaria, Ch. Chen, X. Jiang, A. Yu, Phys. Chem. Chem. Phys. 16 (2014) 11471–11480.
[32] S. Cho, J.-W. Jang, J.S. Lee, K.-H. Lee, Langmuir 26 (17) (2010) 14255–14262.
[33] T.-Q. Liu, O. Sakurai, N. Mizutani, M. Kato, J. Mater. Sci. 21 (1986) 3698–3702.
[34] N.S. Ramgir, D.J. Late, A.B. Bhise, M.A. More, I.S. Mulla, D.S. Joag, K. Vijayamohanan, J. Phys. Chem. B 110 (2006) 18236–18242.
[35] M. Shoeb, B.R. Singh, J.A. Khan, W. Khan, B.N. Singh, H.B. Singh, A.H. Naqvi, Adv. Nat. Sci.: Nanosci. Nanotechnol. 4 (2013) 035015–035026.

[36] G. Applerot, A. Lipovsky, R. Dror, N. Perkas, Y. Nitzan, R. Lubart, A. Gedanken, Adv. Funct. Mater. 19 (2009) 842–852.
[37] M.-L. Kaariainen, C.K. Weiss, S. Ritz, S. Putz, D.C. Cameron, V. Mailander, K. Landfester, Appl. Surf. Sci. 287 (2013) 375–380.
[38] N. Padmavathy, R. Vijayaraghavan, Sci. Technol. Adv. (2008), http://dx.doi.org/10.1088/1468-6996/9/3/035004.
[39] L. Zhang, Y. Jiang, Y. Ding, M. Povey, D. York, J. Nanopart. Res. 9 (2007) 479–489.
[40] J. Sawai, E. Kawada, F. Kanou, H. Igarashi, A. Hashimoto, T. Kokugan, M.J. Shimizu, Chem. Eng. Jpn. 29 (4) (1996) 627–633.